Transport Properties of Hydroxide and Proton Conducting Membranes

Michael R. Hibbs,[†] Michael A. Hickner,[‡] Todd M. Alam,[†] Sarah K. McIntyre,[†] Cy H. Fujimoto,[†] and Chris J. Cornelius*,[†]

Sandia National Laboratories, P.O. Box 5800, Mailstop 0734, Albuquerque, New Mexico 87185, and Department of Materials Science and Engineering, The Pennsylvania State University, University Park, Pennsylvania 16802

Received November 15, 2007. Revised Manuscript Received January 2, 2008

Hydroxide anion conducting solid polymer membranes, also termed anion exchange membranes, are becoming important materials for electrochemical technology, and activity in this field, spurred by renewed interest in alkaline fuel cells, is experiencing a resurgence. Solid polymer anion exchange membranes enable alkaline electrochemistry in devices such as fuel cells and electrolyzers and serve as a counterpoint to proton exchange membranes, of which there is a large body of literature. For their seeming importance, the details of transport in alkaline exchange membranes has not been explored thoroughly. In this work, a chloromethylated polymer with a polysulfone backbone was synthesized. ^{1}H NMR spectroscopy was performed to determine the chloromethyl content and its position on the polymer structure. The chloromethylated polymer was solution cast to form clear, creasable films, and subsequent soaking of these films in aqueous trimethylamine gave benzyltrimethylammonium groups. The resulting anion exchange membranes swell in water and show varying degrees of ionic conductivity depending on their ion exchange capacity. The water mobility in the anion exchange membranes was greater than in previously studied proton exchange membranes; however, the transport properties in these new materials were lower than what might have been expected from the water behavior. This comparison gives some insight as to future anion exchange membrane design objectives.

Introduction

Historically, anion-exchange membranes (AEMs) have been used mainly in electrodialysis for the desalination of brackish water and for the production of table salt from seawater.[1] In recent years, however, interest has grown in their application toward more demanding uses such as alkaline fuel cells and electrolyzers due to the low overpotentials associated with many electrochemical reactions at high pH[2,3] and the potential to forego noble metal catalysts.[4] Unlike cation exchange membranes where highly chemically stable perfluorinated membranes such as Nafion (DuPont) and Flemion (Asahi Glass) dominate the market, commercially available AEMs are typically based on cross-linked polystyrene and are not very stable in alkaline or electrochemical environments. In addition, the aminated cross-linked polystyrene is blended with other polymers and fabric supports that limit ionic conductivity and may decrease the chemical stability of the membrane. Thus, there is a need to develop new AEMs that not only have high conductivity and ion selectivity but that also exhibit excellent chemical stability at high pH and elevated temperatures.

AEMs based on the polysulfone, Udel 1700 (Amoco), were initially reported by Zschocke and Quellmalz, who described the material's alkaline stability and demonstrated its use in electrodialysis.[5] Their AEMs were prepared by chloromethylation of the parent polysulfone followed by exposure to trimethylamine to form benzyltrimethylammonium groups. Sata et al. later compared a series of AEMs prepared by aminating with various tertiary amines and determined that those made with trimethylamine were the most stable.[6] Bauer et al. prepared AEMs from the same chloromethylated polysulfone by aminating with a bis-tertiary amine, 4,4′-diazabicyclo-[2.2.2]-octane, and concluded that the resulting membranes were more stable under alkaline conditions than membranes with benzyltrialkylammonium groups.[7] Hao et al. have reported making cross-linked AEMs by treating films of chloromethylated polysulfone with diamines to control properties such as water swelling, permselectivity, and conductivity.[8] Hwang and Ohya prepared multiblock copolymers containing polysulfone blocks which were then chloromethylated and treated with trim-

* Corresponding author. E-mail: cjcorne@sandia.gov.
[†] Sandia National Laboratories.
[‡] The Pennsylvania State University.

(1) Davis, T. A.; Genders, J. D.; Pletcher, D. *A First Course in Ion Permeable Membranes*; Electrochemical Consultancy: Romsey, 1997.
(2) Varcoe, J. R.; Slade, R. C. T. *Fuel Cells* **2004**, *4*, 1.
(3) Kordesch, K.; Olivera, J. C. T. *Int. J. Hydrogen Energy* **1988**, *13*, 411.
(4) Varcoe, J. R.; Slade, R. T. C.; Wright, G. L.; Chen, Y. *J. Phys. Chem. B* **2006**, *110*, 21041.
(5) Zschocke, P.; Quellmalz, D. *J. Membr. Sci.* **1985**, *22*, 325.
(6) Sata, T.; Tsujimoto, M.; Yamaguchi, T.; Matsusaki, K. *J. Membr. Sci.* **1996**, *112*, 161.
(7) Bauer, B.; Strathmann, H.; Effenberger, F. *Desalination* **1990**, *79*, 125.
(8) Hao, J. H.; Chen, C.; Li, L.; Yu, L.; Jiang, W. *Desalination* **2000**, *129*, 15.

10.1021/cm703263n CCC: $40.75
Published on Web 03/11/2008

ethylamine to form AEMs.[9,10] They reported the formation of macroreticular structures within their membranes which led to improved electrochemical properties.

McGrath and co-workers have prepared proton exchange membranes (PEMs) based on a polysulfone made from the condensation polymerization of 4,4′-biphenol and a 4,4′-dihalodiphenylsulfone.[11,12] This type of ion-containing polymer can be prepared from sulfonated monomers, or sulfonic acid groups can be attached to the parent polysulfone after polymerization. Films of these materials can be easily cast to give robust membranes with high ionic conductivities and excellent water transport properties. These materials (particularly those made from sulfonated monomers) have been widely studied in fuel cell applications and represent the state of the art in hydrocarbon-based PEMs.[13] We have chosen to build upon this work for the study of AEMs due to the base polymer's chemical stability and film-forming characteristics.

This paper describes the synthesis of a series of AEMs based on polysulfone backbones and the comparison of these AEMs to PEMs based on a polyphenylene backbone[14] that this group has studied in the past. The unfunctionalized polysulfone was prepared and then functionalized by adding ionic groups to the polymer backbone in two reaction steps. These quaternary ammonium functionalized membranes were then compared to the sulfonated polyphenylene membranes in terms of water uptake, ion conductivity, effective water self-diffusion coefficient, and pressure-driven water permeability.

Experimental Section

Materials. All reagents were purchased from commercial vendors and used without further purification unless specified. The unfunctionalized polysulfone (PS) was prepared as described by Harrison et al.[15] The sulfonated poly(phenylene) (SDAPP) was prepared as described by Fujimoto et al.[14]

Characterization and Measurements. Gel permeation chromatography (GPC) was performed with a liquid chromatograph equipped with a Viscotek VE2001 isocratic pump and autosampler and a Viscotek VE3580 refractive index detector. The mobile phase was tetrahydrofuran, and the system was operated at 25 °C with a flow rate of 1.0 mL min^{-1}. The weight-average molecular weights were measured by calibration with polystyrene standards.

^{1}H NMR spectra of the polymers were obtained on a Bruker spectrometer using 5 mm o.d. tubes. Sample concentrations were about 5% (w/v) in $CDCl_3$ containing 1% TMS as an internal reference. Pulsed-field gradient diffusion measurements were obtained using a 5 mm broadband gradient probe on a Bruker spectrometer. The water self-diffusion constant was measured using a pulsed field gradient stimulated echo (PFG STE) sequence. The gradient was varied in 16 steps from 2% to 95% of the maximum gradient strength, 54.5 G cm^{-1}. For the STE diffusion experiment, the decay of the signal intensity, $S(T + 2\tau)$, is given by

$$S(T+2\tau_1) = \frac{S_0}{2}\exp(-2\tau_1/T_2 - T/T_1)\exp[-D_{\text{eff}}\gamma^2 g^2\delta^2(\Delta - \delta/3)] \quad (1)$$

where S_0 is the initial signal intensity, T and τ_1 are interpulse spacings, T_1 is the spin–lattice relaxation time, T_2 is the spin–spin relaxation time, D_{eff} is the effective diffusion coefficient (m^2 s^{-1}), γ is the gyromagnetic ratio of the observed nuclei, g is the gradient strength, δ is the length of the gradient pulse, and Δ is the diffusion time. In these diffusion experiments the gradient pulse length δ was 2 ms, while Δ was fixed at 50 ms for all samples. The effective water self-diffusion coefficient (D_{eff}) was obtained by fitting the experimental data to the above equation. All samples were removed from solution—lightly patted dry, placed in an NMR tube, and immediately placed in the spectrometer for measurement. A saturated cotton plug was also included in the tube (outside of the probe coil) to maintain the relative humidity in the NMR tube as close to saturation as possible.

Hydroxide anion conductivity of the membranes was measured by two-probe electrochemical impedance spectroscopy (EIS) using a Solartron 1260 frequency response analyzer coupled to a Solartron 1287 potentiostat. EIS was performed on water-immersed samples at 30 °C as described in ref 14.

Ion exchange capacities (IEC) were determined by a back-titration. Membranes (in hydroxide form) were immersed in 100 mL of 0.1 M HCl standard for 48 h. The solutions were then titrated with a standardized NaOH solution. Control samples (with no membranes) were also titrated with NaOH, and the difference between the volume required to titrate the sample and the control was used to calculate the amount of hydroxide ions in the membranes. After titration the membranes were washed with water and soaked in 1 M HCl solution for 48 h to convert them to their chloride form. They were then soaked in water for 24 h to remove any remaining HCl, and then the wet mass of each membrane was determined by wiping the excess water from the surface and weighing. The membranes were then dried under vacuum in the presence of P_2O_5 at room temperature for 24 h and then reweighed to determine the dry mass. The membranes were converted to chloride ion form prior to drying to avoid degradation of the benzyltrimethyl ammonium groups by hydroxide ions. Thus the IEC is expressed as milliequivalents (of hydroxide ions) per gram of dry membrane (in the chloride ion form). Water uptake values were calculated as the difference in the hydrated and dry masses of a membrane divided by the mass of the dry chloride form as detailed in ref 14.

Differential scanning calorimetry (DSC) was performed using the same methods as in ref 16 to quantify the enthalpy of melting (ΔH_m) of water in the membrane samples. Pressure-driven water flux was measured using a high-pressure dead-end stirred cell (Sterlitech, Kent, WA). The amount of water that permeated through the membrane was recorded versus time using an electronic balance with data acquisition capability. The water flux through the membrane was computed from the linear slope of the change in water mass with time curve at a zgiven pressure, typically 200 psi. The permeability was computed by normalizing the flux for pressure and membrane thickness as given by

$$P_{H_2O} = \frac{dm_{H_2O}}{dt}\frac{l}{A_m \Delta p} \quad (2)$$

where $P_{H_2}O$ is the water permeability (g s^{-1} cm^{-2} psi^{-1} μm), $dm_{H_2}O/dt$ is the slope of the linear portion of the mass versus time

(9) Hwang, G.-J.; Ohya, H. *J. Membr. Sci.* **1998**, *140*, 195.
(10) Hwang, G.-J.; Ohya, H. *J. Membr. Sci.* **1998**, *149*, 163.
(11) Wang, F.; Hickner, M.; Kim, Y.-S.; Zawodzinski, T. A.; McGrath, J. E. *J. Membr. Sci.* **2002**, *197*, 231.
(12) Wang, F.; Hickner, M.; Ji, Q.; Harrison, W.; Mecham, J.; Zawodzinski, T.; McGrath, J. E. *J. Macromol. Symp.* **2001**, *75*, 387.
(13) Hickner, M. A.; Ghassemi, H.; Kim, Y.-S.; Einsla, B. R.; McGrath, J. E. *Chem. Rev.* **2004**, *104*, 4587.
(14) Fujimoto, C. H.; Hickner, M. A.; Cornelius, C. J.; Loy, D. A. *Macromolecules* **2005**, *38*, 5010.
(15) Harrison, W. L.; Wang, F.; Mecham, J. B.; Bhanu, V. A.; Hill, M.; Kim, Y. S.; McGrath, J. E. *J. Polym. Sci., Part A: Polym. Chem.* **2003**, *41*, 2264.
(16) Hickner, M. A.; Fujimoto, C. H.; Cornelius, C. J. *Polymer* **2006**, *47*, 4238.

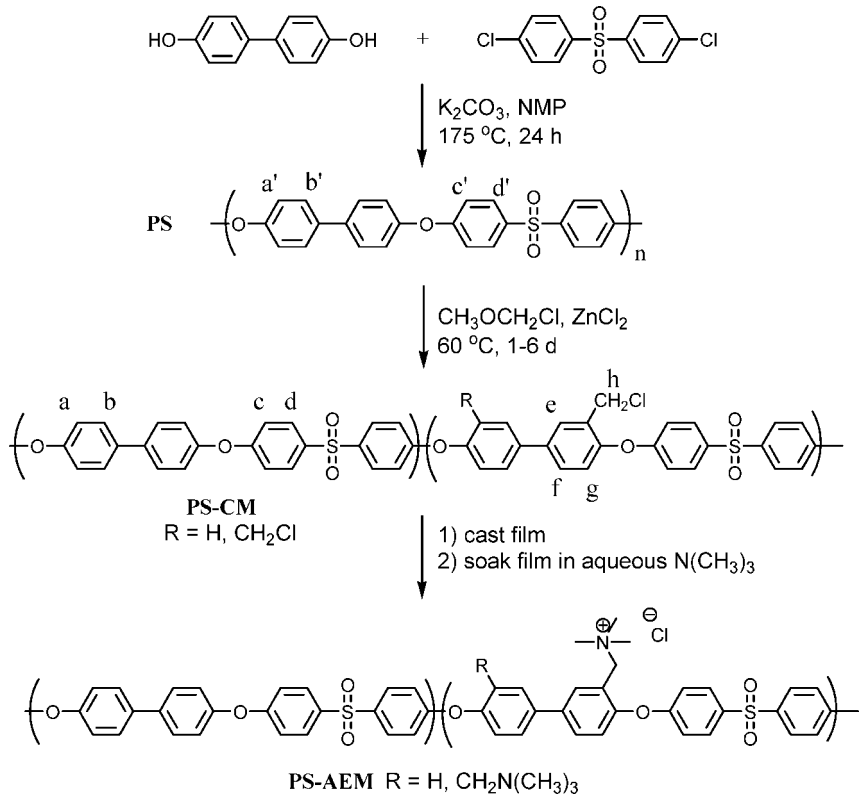

Figure 1. Synthesis of PS and chloromethylation to form PS-AEMs.

curve (g s^{-1}), A_m is the area of the membrane (cm^2), l is the thickness of the membrane (μm), and Δp is the transmembrane pressure (psi). Typical membrane samples were between 30 and 50 μm thick.

Synthesis of PS-CM. Polymers were prepared with various degrees of chloromethylation. The procedure for preparing PS-CM with 1.25 $-CH_2Cl$ groups per repeat unit is described. PS (18.02 g) was dissolved in 450 mL 1,1,2,2-tetrachloroethane in a two-necked flask equipped with a magnetic stir bar and a condenser under nitrogen. A mixture of dimethoxymethane (199 mL, 2.2 mol) and 180 mL of 1,1,2,2-tetrachloroethane was slowly added over 30 min followed by addition of $SOCl_2$ (82 mL, 1.1 mol). A solution of $ZnCl_2$ (6.13 g, 45 mmol) in 45 mL of THF was then added, and the reaction was heated at 60 °C for 5 days. After cooling to room temperature the reaction was poured into methanol (2 L). The precipitate was collected by filtration, dissolved in 300 mL of CH_2Cl_2, and reprecipitated into acetone (2 L). The precipitate was collected by filtration and dried under vacuum to yield an off-white solid (17.9 g).

Casting and Amination of Films. Solutions of PS-CM in dimethylacetamide (5–8% w/w) were filtered into glass dishes and placed in a vacuum oven at 50 °C for 24 h. The oven temperature was then increased to 80 °C over 2 h and was held there for 1 h, after which the films were removed from the dishes by immersing them in water. To form the benzyltrimethylammonium functional groups, the films were immersed in a 45% (w/w) solution of trimethylamine in water in a closed container for 48 h at room temperature. They were then soaked in 1 M NaOH for 48 h to exchange the chloride ions for hydroxide ions. Finally, the membranes were immersed in deionized water for at least 24 h prior to analysis.

Results and Discussion

The synthetic scheme for the preparation of the membranes is shown in Figure 1. The chloromethylated polysulfone, PS-CM, was prepared by a chloromethylation reaction on the unfunctionalized parent polymer, PS. To avoid handling the highly toxic reagent chloromethyl methyl ether (CMME), it was generated in situ according to the procedure of Wright et al.[17] during the synthesis of PS-CM. ^{1}H NMR analysis indicated that chloromethylation of PS occurred at the activated positions of the biphenyl moieties and that the chloromethylation reaction occurred a maximum of once on each aryl ring in the biphenyl unit (Figure 2). One functional group per aryl ring can be explained by both the steric and electron withdrawing effects of a chloromethyl group which would prevent addition of a second group on the same ring. Figure 2 clearly shows that as the degree of functionalization (DF) of PS-CM is increased, the peaks for the protons in the biphenyl units (a′ and b′) decrease in size, and three new peaks of equal intensity (e, f, and g) arise in the aryl region. The intensities of each of these new aryl peaks is half that of the new peak from the two protons in the newly formed chloromethyl group (h) which appears at 4.6 ppm and increased in size as the DF increased. The extent of chloromethylation was determined by an analysis of the ^{1}H NMR spectra in which the integrals of the signals from the $-CH_2Cl$ groups were compared to the sum of the integrals of the signals from all aromatic protons.

Table 1 summarizes the reaction conditions and results for seven different batches of PS-CM. In all cases, the reaction temperature was 60 °C and 1 equiv of $ZnCl_2$ was added as catalyst. As the data shows, the reaction was rather slow and required a large excess of chloromethylating reagent

(17) Wright, M. E.; Toplikar, E. G.; Svejda, S. A. *Macromolecules* **1991**, *24*, 5879.

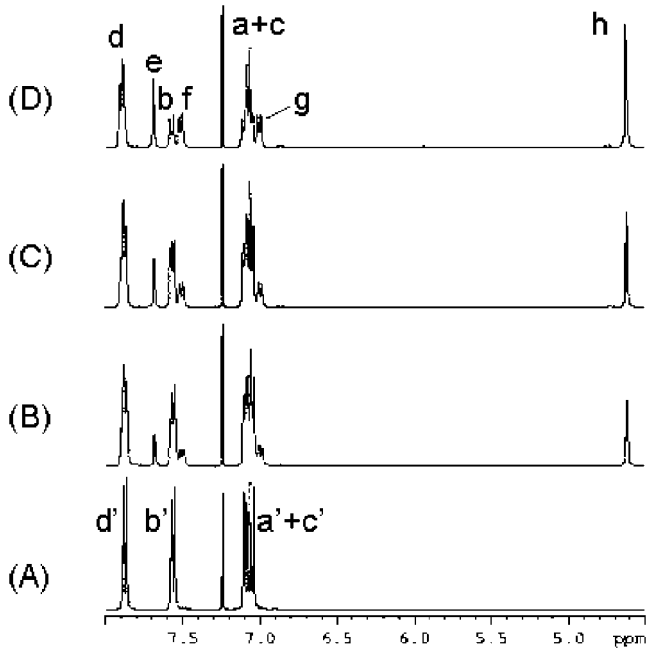

Figure 2. Expanded regions of ^{1}H NMR spectra of PS-CM with (A) DF = 0, (B) DF = 0.63, (C) DF = 0.83, and (D) DF = 1.41. The peak at 7.24 ppm is from the chloroform solvent.

Table 1. Chloromethylation Reaction Conditions and Molecular Weight Results

sample	equivalents of CMME	time (h)	DF[a]	$M_n \times 10^3$ (g mol^{-1})	$M_w \times 10^3$ (g mol^{-1})	PD
1	20	48	0.42	57	125	2.2
2	50	42	0.63	56	118	2.1
3	50	68	0.83	49	129	2.6
4	50	54	0.89	52	119	2.3
5	50	85	1.18	48	119	2.5
6	50	72	1.21	62	131	2.1
7	63[b]	137	1.37	53	121	2.3

[a] Degree of functionalization = (number of chloromethyl groups/repeat unit). [b] Initially, 50 equiv were added to the reaction. After 48 h, an additional 13 equiv were added.

and nearly six days for the number of chloromethyl groups per polymer repeat unit to reach 1.37. Molecular weight data for batches of PS-CM are also given in Table 1. The weight-average molecular weights of these seven batches ranged from 118 000 g mol^{-1} to 131 000 g mol^{-1}. The polydispersities (PD) were all near 2, a typical value for condensation polymerizations.

Attempts to chloromethylate PS in other chlorinated solvents such as chloroform or 1,2-dichloroethane failed as a result of precipitation of the polymer upon addition of the chloromethylating reagents. Reaction temperatures higher than 60 °C, reaction times longer than 6 days, or use of $SnCl_4$ as the catalyst resulted in gels, presumably because of cross-linking via Friedel–Crafts alkylation by the chloromethyl groups in the presence of a Lewis acid.

Films of PS-CM were prepared by casting dimethylacetamide (DMAc) solutions under vacuum at elevated temperatures, up to 80 °C. These films were then immersed in an aqueous solution of trimethylamine to form the quaternary ammonium functional groups by substitution of the chlorine atoms in the chloromethyl groups (Figure 1). As the ionic groups were formed, the membranes became hydrophilic and swelled to an extent that depended on the number of ionic groups. Soaking in aqueous media also ensured that any residual DMAc from the casting procedure was removed from the membranes. Prepared this way, the aminated PS membranes (PS-AEM) were in chloride form (the quaternary amine counterions were chloride ions). To convert them to hydroxide form, the membranes were immersed in an excess of 1 M NaOH(aq) at room temperature for two days.

Table 2. Theoretical and Measured Ion Exchange Capacities of Membranes

	IEC (mequiv g^{-1})	
sample	theoretical[a]	measured
1	0.94	0.69
2	1.36	1.04
3	1.69	1.40
4	1.79	1.46
5	2.24	1.66
6	2.28	1.82
7	2.50	1.89

[a] Calculated from DF assuming complete amination, ion exchange, and water removal upon drying.

Following their conversion to the hydroxide form, these membranes have a yellow color and are tough and flexible. This is in contrast to many commercially available AEMs, such as Tokuyama's AMX and AM1 membranes which change color from light yellow to black after less than an hour of exposure to 1 M NaOH. This color change in commercial membranes is presumably due to dehydrochlorination of poly(vinyl chloride) which is blended with the ionomeric component for mechanical stability. Needless to say, this chemical degradation weakens the membranes and renders them unusable in high pH applications. Tokuyama also makes an alkaline stable Neosepta AHA membrane which does not change color in 1 M NaOH, although it is reported by the manufacturer to have a lower chloride ion conductivity (4–5 mS cm^{-1}) than the AMX and AM1 membranes (5–6 and 7–11 mS cm^{-1}, respectively).

As can be seen in Table 2, the measured IEC values were all lower than the theoretical IEC values (based on DF assuming 100% amination efficiency, 100% conversion to hydroxide form, and 100% water removal when drying). The values determined by titration were between 73% and 83% of the calculated values. This could be due to incomplete conversion of chloromethyl groups to quaternary ammonium groups, incomplete exchange of chloride ions for hydroxide ions in the step prior to titration, or incomplete drying of the membranes after the titration. Samples dried for more than 24 h did not show any additional mass loss, so 24 h was assumed to be enough time to completely dry the membranes. Ion exchange by soaking for longer than 48 h or in >1 M NaOH did not have a significant effect on the measured conductivities or IEC values so the replacement of chloride ions with hydroxide ions appears to be complete. Thus the most likely cause for the differences between theoretical and measured IEC values is incomplete amination. In any case, the differences were small enough to be tolerated in this study, and the measured IEC values all increased in a trend that was consistent with increasing theoretical IEC values.

Water uptake and ionic conductivity for the membranes over a range of IEC values are shown in Figure 3. It can be seen that at low IEC values (<1.5 mequiv g^{-1}), the water

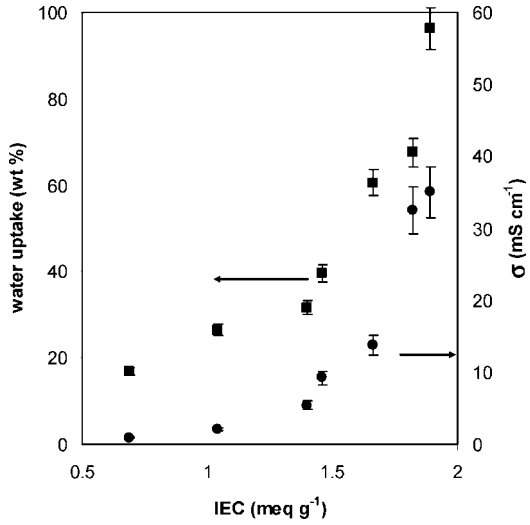

Figure 3. Water uptake and hydroxide anion conductivity versus ion exchange capacity; (■) water uptake; (●) conductivity.

uptake increased in a linear fashion with increasing IEC. This moderate increase is due to the ionic groups being distributed throughout the film and only being able to form small hydrated regions around the ions. These small hydrated regions are surrounded by a large volume fraction of unfunctionalized polymer which prevents significant swelling or ion transport. At higher IEC values (>1.5 mequiv g^{-1}), the water uptake increased sharply at a proportional rate larger than that observed for lower IEC values, due to the hydration regions near the ions overlapping and the decreased volume fraction of the unfunctionalized phase. The high molecular weights of the parent polymers yielded mechanically robust membranes even for highly swollen samples, and no gel-like mechanical properties were observed for any of the samples in this study. Figure 3 emphasizes the need to attain high IEC values for this type of chloromethylated polysulfone system to achieve sufficient conductivity. Typical synthetic conditions and reaction times yielded materials with IECs less than 1.5 mequiv g^{-1}. Much longer reaction times and careful monitoring of the reaction conditions were needed to realize membranes with high hydroxyl anion conductivity, for example, above 30 mS cm^{-1}.

The hydroxide ion conductivities of the PS-AEMs showed a trend that was similar to that for water uptake. At low IEC values, the conductivity of the membranes was rather low and increased in a gradual, linear fashion. In this regime, conductivity is thought to be limited by the connection between ionic domains, and as the IEC value increases, the conductivity increases rapidly as the volume fraction of water and concentration of ionic groups in the membrane increases. The trends in water uptake and ion conductivity for the PS-AEMs are reminiscent of sulfonated proton exchange membranes (PEMs), where a large body of literature exists, so further investigation of their properties is warranted. The water uptake for the membranes is plotted in Figure 4 as a function of ion exchange capacity. The water uptake curve as a function of IEC for PS-AEMs and a sulfonated poly(phenylene) (SDAPP) membrane is nearly identical, and in addition, the water uptake of SDAPP PEMs had previously been shown to be comparable to that of polysulfone-based

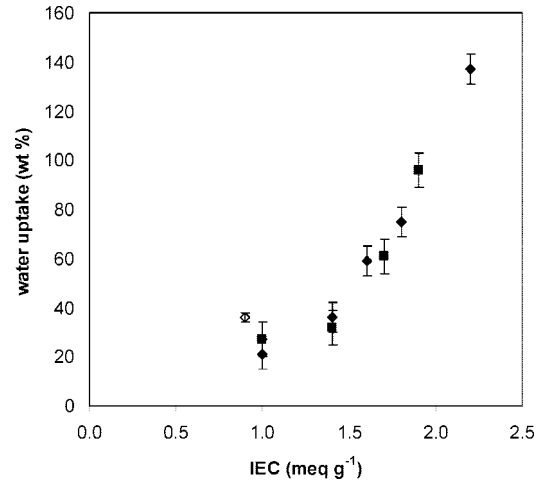

Figure 4. Water uptake as a function of IEC for all membranes: (◇) Nafion, (■) PS-AEM, and (◆) SDAPP.

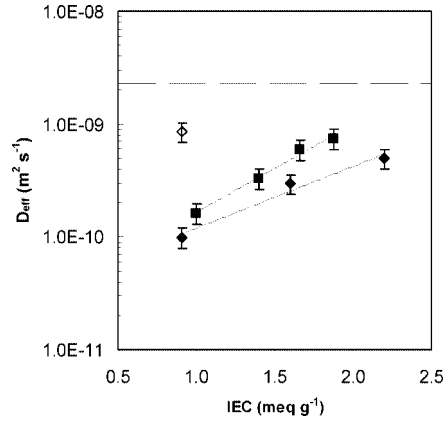

Figure 5. Effective water self-diffusion coefficient at 25 °C (Δ = 50 ms) in the membrane as a function of ion exchange capacity: (◇) Nafion, (■) PS-AEM, (◆) SDAPP, and (dashed line) liquid bulk water.

sulfonated PEMs.[14] Polysulfone and polyphenylene backbones have very high T_g values and most likely similar chain stiffness characteristics which may lead to similar water uptakes. Nafion is based on a more flexible carbon−carbon bonded perfluorinated backbone which gives a slightly higher water uptake than the others at low ion exchange capacity. Nafion is generally not available in higher ion exchange capacities due to its solubility in water. This underscores the major differences between poly(perfluorosulfonic acid) and hydrocarbon ion exchange membranes.

The effective water self-diffusion coefficients in the membranes measured using PFG-NMR are plotted in Figure 5 as a function of ion exchange capacity. This data shows that the water diffuses much faster in Nafion than in SP-AEM or SDAPP at low ion content. The effective water self-diffusion coefficients (D_{eff}) for SP-AEM and SDAPP increase with an increase in ion exchange capacity and approach the value for Nafion at the highest IECs. The D_{eff} in Nafion is still 2.5 times lower than the bulk water self-diffusion coefficient (2.3 × 10^{-9} m^2 s^{-1} at 25 °C[18]), indicating that on average, water diffusion in these types of membranes is still much slower than in bulk water. Over the entire range

(18) Mills, R. *J. Phys. Chem.* **1973**, *77*, 685.

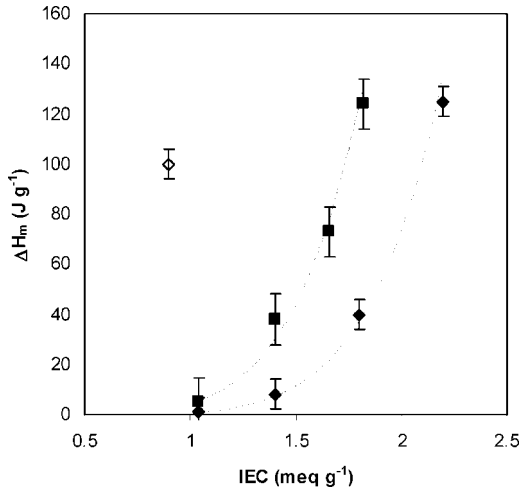

Figure 6. Apparent enthalpy of melting for water in the membrane as a function of ion exchange capacity: (◇) Nafion, (■) PS-AEM, and (◆) SDAPP.

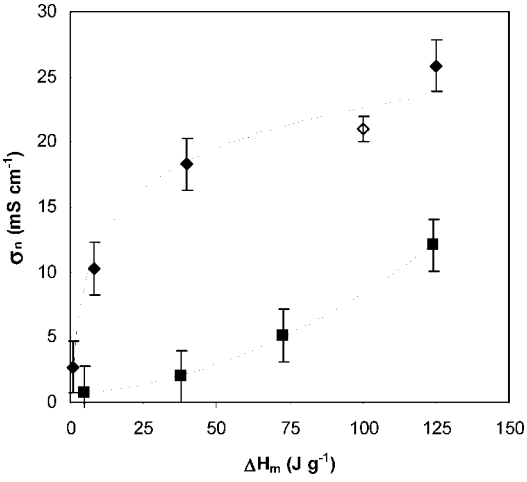

Figure 7. Normalized conductivity as a function of the apparent enthalpy of melting: (◇) Nafion, (■) PS-AEM, and (◆) SDAPP.

of IECs, the D_{eff} in PS-AEMs is greater than that of water in SDAPP. This suggests that the water is moving faster in the PS-AEMs and is less bound within the polymer than it is in the SDAPP polymers. Differential scanning calorimetry results in Figure 6 support the NMR data. The enthalpy of melting of water in the SDAPP membranes is lower than for the PS-AEMs for a given IEC. A higher enthalpy of melting is akin to the water being more loosely bound within the polymer structure and more free to move as shown in the self-diffusion coefficient measurements. Additionally, the enthalpy of melting of water in Nafion is much greater than for the other two polymer families at low ion exchange capacity similar to the PFG-NMR results. These two complimentary measures of water mobility or binding, PFG-NMR and DSC, seem to indicate that the water is less confined, geometrically or chemically, in PS-AEMs than in SDAPP PEMs. It is known that water interacts more strongly with cations than anions in solution.[19] It is possible that this interaction could account for the water binding behavior solely on a chemical basis. Moreover, the strong acid in sulfonated proton exchange membranes yields more free ions in PEMs which require waters of hydration, which may bind water more strongly than the relatively weak base in AEMs. Because there are not as many ion pairs dissociated in AEMs, the absorbed water is less bound within the polymer structure and more free to diffuse. Morphology of the hydrated phase, which is discussed later, may also play a role in the observed water behavior.

It has been shown previously that the behavior of water is tied to the transport properties of PEMs.[14,20,21] To compare the conductivity between the two families of membranes, H^+ versus OH^- mobile species, the ionic conductivity in each case was divided by the mobile ion's mobility in dilute solution:

$$\sigma_n = \frac{\sigma_i}{\mu_i}$$

where σ_n is the normalized conductivity, σ_i is the measured ionic conductivity, and μ_i is the ion's mobility in dilute solution ($H^+ = 4.76$ and $OH^- = 2.69$ relative to K^+).[22,23] The concentration of ions in the membrane is approximately 1–2 M. Admittedly, this concentration is right on the border of the dilute solution limit. For instance, for a pK_a of -1 (e.g., toluene sulfonic acid), 99% of the charges are dissociated in a 1 M solution while only 92% of the charges are dissociated in a 2 M solution which is illustrative of where dilute solution approximations might apply. While normalizing the measured ionic conductivities by the dilute solution ionic mobility is an estimate, we believe this representation of the data helps further the understanding of these membranes. The mobility-normalized conductivity for the membranes in this study as a function of the enthalpy of melting of water in the membranes is shown in Figure 7. A somewhat smooth curve can be drawn through the SDAPP and Nafion points, and it appears as though the conductivity of protons in these two different membranes is tied directly to the water melting behavior in the membrane. However, the mobility correction for H^+ versus OH^- ion transport cannot account for the total difference in behavior between the PEM and AEM classes of materials. Conductivity of ions is a function of both the ion mobility and the concentration of charge carriers. The PEMs and AEMs have similar water uptake as a function of IEC which leads to similar bulk concentrations of potential charge carriers in each case. The major difference in conductivity between proton conducting membranes and hydroxyl conducting membranes in this study can be rationalized by considering the number of mobile carriers or the dissociation of the sulfonate and quaternary amine functional groups. Sulfonic acids are considered strong acids, and the pK_a of aryl sulfonic acid which is the basic unit of SDAPP has been estimated to be on the order of -1.[24] Quaternary amines are weak bases with a pK_b on the order of 4. The dissociation of weak basic groups attached to a

(19) Ayala, R.; Martiñez, J. M.; Pappalardo, R. R.; Sañchez Marcos, E. *J. Phys. Chem. A* **2000**, *104*, 2799.
(20) Hickner, M.; Pivovar, B. *Fuel Cells* **2005**, *5*, 213.
(21) Kim, Y. S.; Dong, L.; Hickner, M.; Glass, T. E.; McGrath, J. E. *Macromolecules* **2003**, *36*, 6281.
(22) Dean, J. A. *Lange's Handbook of Chemistry*, 15th ed.; McGraw-Hill: New York, 1999.
(23) Vanysek, P. Ionic conductivity and diffusion at infinite dilution. In *CRC Handbook of Chemistry and Physics*, 83rd ed.; Lide, D. R., Ed.; CRC Press: Boca Raton, 2002.
(24) Kreuer, K. D. *J. Membr. Sci.* **2001**, *185*, 29.

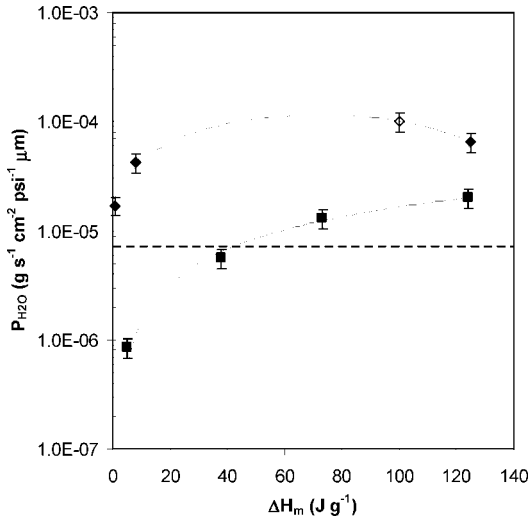

Figure 8. Pressure-driven water permeability as a function of the apparent enthalpy of melting: (◇) Nafion, (■) PS-AEM, and (◆) SDAPP.

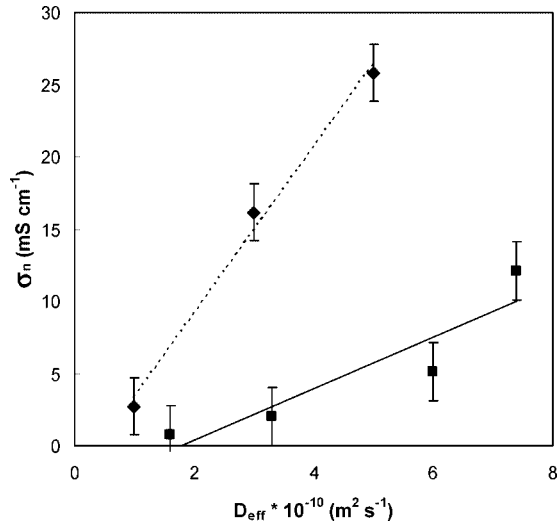

Figure 9. Normalized ionic conductivity (to OH^- and H^+ dilute solution mobility, respectively) versus effective water diffusion coefficient determined by PFG NMR for (■) PS-AEM and (◆) SDAPP membranes. Dashed lines indicate linear slopes of 6 (mS cm^{-1}/m^2 s^{-1}) for SDAPP samples and 2 (mS cm^{-1}/m^2 s^{-1}) for PS-AEM samples.

polymer chain presents a considerable theoretical barrier for efficient hydroxide anion conduction in these types of systems. Given what is known about the empirical upper limit of proton conductivity in practical PEMs, for example, on the order of 10^{-1} S cm^{-1}, the prospect of meeting or exceeding this perceived limit for hydroxyl anion conduction is small given functionalized polymer approach for OH^- conduction.

Pressure-driven water permeability was measured to compliment the conductivity studies. Ion conductivity and water flux occur in response to different driving forces (potential gradient versus pressure gradient), and their comparison can provide insight into hydrated transport domains in the membranes. The water permeability for the membranes as a function of water binding from DSC is shown in Figure 8. As with conductivity, the water permeability through PEMs is significantly greater than for AEMs across the entire range of materials. The data in Figures 5− present an interesting picture of transport in these classes of materials. While water is more mobile (less bound) in AEMs as measured by PFG-NMR and DSC, transport of ions and water in these systems is slower. Taken together with the water mobility and binding data, the conductivity and permeability measurements may indicate that there is a significant amount of phase separation in the PEMs which does not exist in the AEMs. Nafion has a more organized nanophase morphology than the SDAPP membranes as shown previously, which promotes higher conductivity and methanol permeability for a given ion exchange capacity.[16] More loosely bound water in these systems leads to higher rates of transport. This does not seem to be the case when comparing transport in PEMs with that in AEMs. While water is very mobile in AEMs, as shown by PFG-NMR and DSC, both the conductivity and the water permeability are less than what would be expected. The lower conductivity is understandable when considering the dissociation of quaternary amines as compared to aryl sulfonates, but the water permeability results are counterintuitive.

Morphological organization or lack thereof in each membrane type may have been anticipated by considering the method in which the membranes were formed. The SDAPP PEMs were solution cast in their sodium neutralized yet still ionic form. These conditions allowed the ionic groups to aggregate in the solid-state membrane. The PS-AEMs were cast in their chloride, nonionic form where there is no driving for ionic aggregation or phase separation during the casting process. Therefore, PEMs show the behavior of having hydrated transport pathways or domains, where the AEMs behave more like a swollen gel. The transport is tied to the water mobility in each case, but hydrated domains give faster transport rates for a given degree of water binding.

This impact of polymer morphology can be seen in Figure 9, in which the membrane conductivity versus D_{eff} is plotted. In general, there is a linear increase in the proton conductivity with increased water diffusion rates, consistent with the conductivity being significantly influenced by the water transport properties. Inspection of Figure 9 also shows that this variation in conductivity is very different for the PS-AEM and SDAPP membranes. For the PS-AEM membranes the variation is 2 (mS cm^{-1}/m^2 s^{-1}), while for the SDAPP membranes the variation is more dramatic with a 6 (mS cm^{-1}/m^2 s^{-1}) variation. This difference in conductivity behavior with water diffusion rates along with the water permeability data reflects the impact that the local differences in the polymer morphology and structure must play on the membrane performance. These results also support the argument that simply designing membranes that have increased water mobility (D_{eff}) will not necessarily improve conductivity performance.

Conclusions

Novel AEMs have been synthesized from a chloromethylated polysulfone. By controlling the degree of functionalization on the polymers, AEMs with a wide range of water uptake values and ionic conductivities can be prepared. The transport properties of PS-AEMs were compared with those of sulfonated polyphenylenes and Nafion. It was found that

although the self-diffusion coefficient for water in the membrane is greater and water binding is lower in PS-AEMs, their transport properties in terms of ion conductivity and pressure-driven water permeability were depressed compared to the sulfonated PEMs. This seeming contradiction between the behavior of water and the resulting transport properties was rationalized by considering the phase-separated morphology of each system. The PS-AEMs were converted to the ionic form after membrane formation. This processing scheme did not allow the ionic groups to form phase separated domains as in membranes that are cast from ionic form polymer. The sulfonated polymers were cast in the ionic form and therefore had some degree of phase separation which promoted high transport rates even though the water diffusion is slower and binding is stronger in these systems probably due to the hydration of the sulfonic acid groups themselves. Further problems exist for creating AEMs with high conductivity due to the relatively weak basicity of quaternary ammonium functional groups and the lower mobility of hydroxyl anions as compared to protons. While proton conductivities of sulfonate functionalized polymeric membranes have been limited to approximately 10^{-1} S cm^{-1}, reaching this value with hydroxyl anion conducting membranes is a serious challenge.

Acknowledgment. Sandia is a multiprogram laboratory operated by Sandia Corporation, a Lockheed Martin Company, for the United States Department of Energy's National Nuclear Security Administration under Contract No. DE-AC04-94AL85000.

Note Added after ASAP Publication. There were errors in Figure captions 4, 5, and 6 in the version published ASAP March 11, 2008; the corrected version published ASAP April 1, 2008.

CM703263N